ELSEVIER

Biophysical Chemistry 121 (2006) 96–104

Biophysical Chemistry

http://www.elsevier.com/locate/biophyschem

Change of the persistence lengths in the conformational transitions of pullulan- and amylose-tricarbanilates

Yoshio Muroga [a,*], Kentaro Hayashi [a], Mitsuhiro Fukunaga [a], Tadaya Kato [b], Shigeru Shimizu [1], Kimio Kurita [1]

[a] *Department of Applied Chemistry, Graduate School of Engineering, Nagoya University, Furo-cho, Chikusa-ku, Nagoya 464-8603, Japan*
[b] *Graduate School of Engineering, Mie University, Tsu, Mie 514-8507, Japan*

Received 11 August 2005; received in revised form 23 November 2005; accepted 21 December 2005
Available online 7 February 2006

Abstract

With raising temperature in the domain of 20 to 60 °C, the intrinsic viscosity [η] for pullulan-tricarbanilate PTC and amylose-tricarbanilate ATC in solutions was found to decrease, indicating that they exhibited thermal-induced conformational transition from expanded form to compact form. The persistence length P_l of the chains, evaluated with small-angle X-ray scattering, has also decreased as the temperature is raised and, moreover, it significantly depended on the solvents employed, where as P_l of pullulan, having no carbanilate groups, has exhibited neither temperature- nor solvent-dependence. The temperature dependence of [η] for PTC and ATC was well elucidated in terms of the temperature-dependent P_l with the wormlike chain model. From these results, it is suggested that intramolecular hydrogen bonds would be formed between carbanilate groups neighboring along the backbone chain, but they are gradually and cooperatively collapsed as the temperature is raised, inducing the conformational transition.

Keywords: Pullulan-tricarbanilate; Amylose-tricarbanilate; Cellulose-tricarbanilate; Pullulan; Wormlike chain; Persistence length; Small angle X-ray scattering

1. Introduction

Temperature dependence of physical properties relating to overall chain-dimension has been measured for cellulose-tricarbanilate (CTC) and amylose-tricarbanilate (ATC) in solutions with various methods [1–5] and it was shown that the polymers exhibit thermal-induced conformational transition from expanded form at low temperature to compact form at high temperature. Moreover, the temperature dependence of the physical properties of some polysaccharide-tricarbanilates was found to depend on the type of bonding between the repeating units, glucopyranoses [4]. From these observations, Sutter and Burchard [4] have suggested that intramolecular hydrogen-bonds might be formed between carbanilate groups neighboring along the backbone chain, and they are cooperatively collapsed as the temperature is raised. Supporting the suggestion of Sutter and Burchard [4], Hsu et al. [6] have analyzed the chain length dependence of the unperturbed dimensions of ATC and CTC with the method of Miller and Flory [7] and found that Zimm–Bragg cooperativity parameter is of the order of 10^{-5} and 10^{-6}, respectively.

If such hydrogen bonds are formed in a polysaccharide-tricarbanilate chain and the chain can be represented by an equivalent wormlike chain model having a persistence length P_l, the conformational transition should be accompanied by a simultaneous change of P_l. Gupta et al. [1,8] indicated that P_l of CTC decreases with raising the temperature, but the temperature dependence of P_l for other polysaccharide-tricarbanilates except CTC has not been fully clarified yet.

In the present work, temperature dependence of intrinsic viscosity [η] for pullulan-tricarbanilate PTC, ATC and CTC in 1,4-dioxane DOX, *N*,*N*-dimethyl formamide DMF and *N*-methyl acetamide NMA solutions was studied in the domain of 20 to 60 °C in order to see whether PTC exhibits the same type

* Corresponding author. Tel./fax: +81 52 789 4822.
E-mail address: ymuroga@apchem.nagoya-u.ac.jp (Y. Muroga).
[1] Permanent address: Faculty of Science and Technology, Nihon University, Chiyoda-ku, Tokyo 101-8308, Japan.

0301-4622/$ - see front matter © 2006 Elsevier B.V. All rights reserved.
doi:10.1016/j.bpc.2005.12.013

of the conformational transition as was observed in ATC and CTC. PTC, ATC and CTC are discriminated from each other in the type of bonding joining the repeating units; original polysaccharide for PTC, pullulan PL, is the α-D-glucan comprising maltotriose repeating units (linked 1,4) connected in 1,6-linkage and those for ATC and CTC, amylose and cellulose, are the 1,4-linked α- and β-D-glucans, respectively. DMF and NMA would have some facility of hydrogen-bond formation and thus affect or break intramolecular hydrogen bonds in the polysaccharide-tricarbanilates.

P_l of PTC and ATC was evaluated at several temperatures with small-angle X-ray scattering SAXS and, in order to find out origin for the conformational transition, the temperature-dependence of $[\eta]$ was analyzed with the temperature-dependence of P_l thus obtained. In general, P_l evaluated from the analysis of SAXS curve or small-angle neutron scattering curve in a comparatively higher scattering-vector region is substantially free from excluded volume effect and effect of the polydispersity of a sample, whereas P_l evaluated from the analysis of physical properties relating to overall chain-dimension tends to be seriously affected by these effects.

2. Experimental

2.1. Materials

Viscosity-averaged molecular-weight M_v of PL (Hayashibara Biochemical Laboratories, Inc., Japan), 1.0×10^5, was estimated from $[\eta]$ in water at 25 °C [9]:

$$[\eta] = 1.91\times10^{-4}\times M_w^{0.67} \quad \text{(in deciliter per gram)} \qquad (1)$$

Nominal M_w/M_n was ca. 2.0.

PTC was prepared by reaction of PL (PF-80, Hayashibara Biochemical Laboratories, Inc., Japan) with phenyl isocyanate in hot pyridine (80–100 °C) [10]. Crude product thus obtained was treated with hot methanol to eliminate biproducts in the reaction and then lower- and higher-molecular-weight fractions were removed by fractionating the product with acetone/water. Degree of substitution (DS) of phenylcarbanilate groups, determined by elemental analysis, was 99.2%±0.8% and $M_v=2.1\times10^5$ was estimated from [η] in DMF at 25 °C [11]:

$$[\eta] = 2.65\times10^{-5}\times M^{0.82} \quad \text{(in deciliter per gram)} \qquad (2)$$

M_w/M_n, 1.2, was determined by GPC, which was registered with a Toyo Soda GPC instrument HLC 802A for THF solutions, using the calibration curve obtained with a series of the standard polystyrene (Toyo Soda Mfg. Co. Ltd.).

ATC and CTC were prepared from amylose (Hayashibara Biochemical Laboratories, Inc., Japan) and cellulose (Asahi Chemical Industry, Co. Ltd., Japan), respectively, by the same procedure as was employed in preparation of PTC. Molecular-weight fractionation was carried out with acetone/ethanol and acetone/water, respectively. M_v of ATC, 6.0×10^4, was estimated from $[\eta]$ in DOX at 20 °C [4]:

$$[\eta] = 2.36\times10^{-5}\times M^{0.88} \quad \text{(in deciliter per gram)} \qquad (3)$$

and M_v of CTC, 5.1×10^4 was estimated from $[\eta]$ in DOX at 20 °C [4]:

$$[\eta] = 3.90\times10^{-5}\times M^{0.90} \quad \text{(in deciliter per gram)} \qquad (4)$$

M_w/M_n was 1.2 and 2.1 for ATC and CTC, respectively, and DS was 99.2%±0.8% for both samples.

Table 1
Observed data and molecular parameters obtained from analysis of SAXS curves for PTC, ATC and PL

Data set	Solvent	Temperature (°C)	C_p (g/dl)	C_p^* (g/dl)	$\langle R_{cs}^2\rangle^{1/2}$ (Å)	q^* (1/Å)	P_l (Å)	
							Method-I	Method-II
(1) PTC								
A	DOX	20	0.69	1.6	5.3±0.5	0.063	45±3.0	45±3.0
B-1	DOX	40	1.00	–	5.3±0.5	0.066	44±3.0	44±3.0
B-2	DOX	40	0.50	–	5.3±0.5	0.066	44±3.0	44±3.0
C	DOX	60	0.69	1.8	5.3±0.5	0.069	42±3.0	42±3.0
D	DMF	20	0.71	1.6	5.3±0.5	0.070	42±3.0	41±3.0
E	DMF	60	0.71	2.2	5.3±0.5	0.082	35±3.0	35±3.0
F-1	NMA	40	1.00	–	5.3±0.5	0.096	32±3.0	30±3.0
F-2	NMA	40	0.50	–	5.3±0.5	0.096	32±3.0	30±3.0
(2) ATC								
A	DOX	20	1.10	2.7	5.3±0.5	0.045	–	64±3.0
B	DOX	60	1.10	3.1	5.7±0.5	0.051	–	56±3.0
C	DMF	20	1.00	3.4	5.3±0.5	0.058	–	49±3.0
D	DMF	60	1.00	4	5.3±0.5	0.064	–	45±3.0
E-1	NMA	40	1.00	–	5.3±0.5	0.090	–	32±3.0
E-2	NMA	40	0.50	–	5.3±0.5	0.090	–	32±3.0
(3) PL								
A-1	WAT	25	0.50	2.3	5.1±1.0	0.132	23±3.0	22±4.0
A-2	WAT	25	1.00	2.3	5.1±1.0	0.132	23±3.0	22±4.0
B	DMF	25	1.00	2.3	5.1±1.0	0.132	23±3.0	22±4.0
C	DMF	60	1.00	2.3	5.1±1.0	0.132	23±3.0	22±4.0

2.2. SAXS experiments and the sample preparation

SAXS experiment was carried out using synchrotron orbital radiation as an X-ray source set up in the Photon Factory of the High Energy Accelerator Organization at Tsukuba, Ibaragi, Japan. The wavelength of the X-ray was 1.488 Å. The scattered intensity $I(q)$ was detected by a position-sensitive proportional counter (PSPC) with 512 channels over a range of 0.01 to 0.25 $Å^{-1}$ in q, where q is the magnitude of the scattering vector, defined by $(4\pi/\lambda)\sin(\theta/2)$ and θ is a scattering angle. The details of the instrumentation and the procedure are described elsewhere [12]. Effects of slit-length and slit-width on the scattering curves could be neglected, because the size of the X-ray beam at sample position was small enough compared with sample to camera distance.

In general, scattering from polymer chain in solution is due to intramolecular-interferences within an isolated polymer chain and intermolecular-interferences between different polymers. However, if polymer concentration C_p is sufficiently lower than the critical concentration C_p^*, above which different solute molecules begin to overlap with each other, the scattering is predominantly due to intramolecular-interferences, except at an extremely small q. C_p^* was estimated with the relation [13,14]:

$$C_p^* = \frac{3M}{4\pi <R_g^2>^{3/2} N_A} \cong \frac{1}{[\eta]}, \tag{5}$$

where M is the molecular weight of polymer and $<R_g^2>$ is the mean-squared radius of gyration of a polymer chain and N_A is the Avogadro's number. The samples for SAXS were prepared so that their C_p would be sufficiently lower than the corresponding C_p^* (Table 1). Therefore, $I(q)$, which was registered on a relative scale, not on an absolute scale, was allowed to be multiplied by a constant factor for comparison with theoretical curves.

2.3. Intrinsic viscosity [η]

Viscosity was measured with Ubbelohde-type capillary viscometer for PTC, ATC and CTC in DOX, DMF and NMA solutions in the temperature domain of 20 to 60 °C. The data was plotted in the forms of Huggins-plot η_{sp}/C_p vs. C_p, Fuoss-Mead plot $\ln\eta_{rel}/C_p$ vs. C_p and Billmeyer plot $\{2(\eta_{sp}-\ln\eta_{rel})\}^{1/2}$ vs. C_p, where η_{sp} and η_{rel} are specific viscosity and relative viscosity, respectively. $[\eta]$ was determined as a common intercept of these plots in the extrapolation of C_p to 0.

3. Theoretical background for treatment of SAXS data

3.1. Evaluation of mean-squared radius of cross-section of a polymer chain, $<R_{cs}^2>$

As is shown below, P_l was evaluated on the basis of scattered intensity $I_{thin}(q)$ for a hypothetical chain with null cross-section. Therefore, it is necessary for evaluation of P_l to convert $I(q)$ to $I_{thin}(q)$.

In general, $I(q)$ for a polymer chain is the product of $I_{thin}(q)$ and cross-sectional factor $I_{cs}(q)$ [15]:

$$I(q) = I_{thin}(q) I_{cs}(q), \tag{6}$$

where $I_{cs}(q)$ is given by:

$$I_{cs}(q) \propto \exp\left(-\frac{1}{2}<R_{cs}^2>q^2\right) \tag{7}$$

For a needle-like molecule,

$$I_{thin}(q) \propto \frac{1}{q} \tag{8}$$

For a semiflexible chain, Eq. (8) does not hold over a whole q range. However, if q is confined to a range,

$$\frac{1}{P_l^2} \ll q^2 \ll \frac{1}{<R_{cs}^2>}, \tag{9}$$

$I_{thin}(q)$ for the chain is still expressed by Eq. (8). That is, when $I(q)$ is plotted in the form of $\ln(I(q)q)$ vs. q^2, it forms

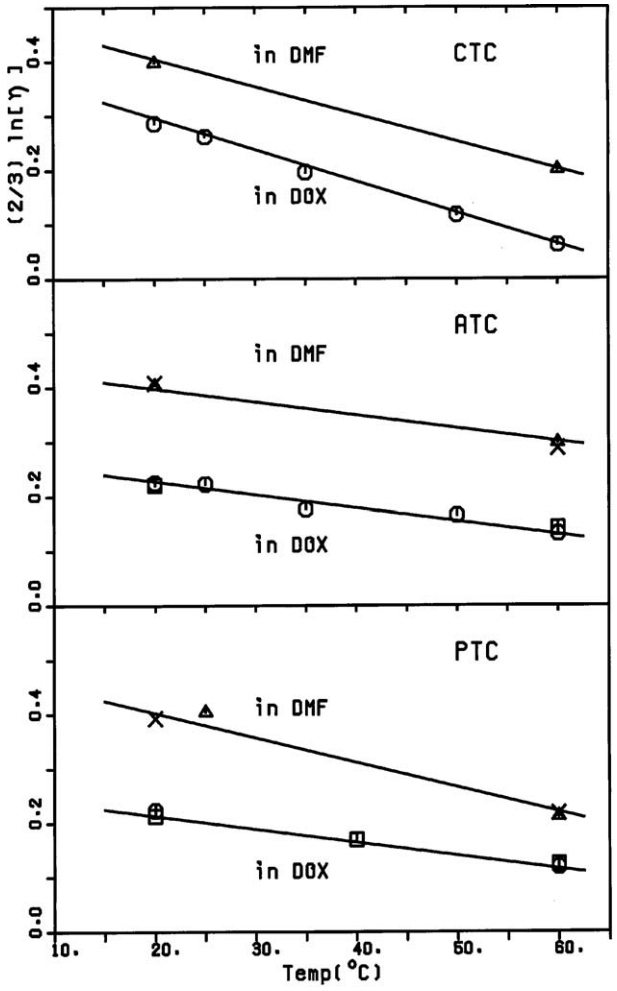

Fig. 1. The temperature T (°C) dependence of $[\eta]$ (dl/g) is shown in the form of (2/3) $\ln[\eta]$ vs. T for PTC, ATC and CTC in DOX solution (○) and DMF solution (△). Symbols square (□) and cross (×) show theoretical dependences of $<R_g^2>_0$ in DOX solution and DMF solution, respectively, which were computed with Eq. (18).

a straight line in the q^2 range of Eq. (9), the slope of which is given by $-1/2\ <R_{cs}^2>$. Once $<R_{cs}^2>$ is thus evaluated, $I_{thin}(q)$ is given by $I(q)\exp(1/2<R_{cs}^2>q^2)$ over a whole q range.

3.2. Evaluation of P_l

P_l of a polymer chain is evaluated on the basis of $I_{thin}(q)$ with Methods -I and -II.

3.2.1. Method-I

In this method, P_l is obtained by comparing $I_{thin}(q)$ with scattering function $P(\theta)$ for a wormlike chain [16]:

$$P(\theta)=\frac{2}{u^2}\{\exp(-u)-1+u\}+\frac{4}{(15L_r)}+\frac{7}{15L_r u}-\left\{\frac{11}{(15L_r)}+\frac{7}{(15L_r u)}\right\}\exp(-u), \quad (10)$$

where parameters u and L_r are related to L and P_l :

$$u=\frac{LP_l q^2}{3} \quad (11)$$

$$L_r=\frac{L}{(2P_l)} \quad (12)$$

Eq. (10) should be applied under the conditions,

$$L_r>10 \quad (13)$$

$$(2P_l q)^2<10 \quad (14)$$

Method-I was recently applied to analyze the local conformations of poly(methacrylic acid) [17] and poly (ethacrylic acid) [18] in aqueous solution.

3.2.2. Method-II

As is well known [19], Kratky plot $I(q)q^2$ vs. q is divided into Guinier-region at $q \ll 1/<R_g^2>^{1/2}$, Debye-region at $1/<R_g^2>^{1/2} \leqq q \leqq 1/P_l$ and Porod region at $1/P_l \leqq q \leqq 1/<R_{cs}^2>^{1/2}$, Eq. (9). In Porod region, scattering is due to rodlike local-structure and thus $I(q)$ is proportional to $1/q$ and the plot $I(q)q^2$ forms a straight line passing through an origin. The

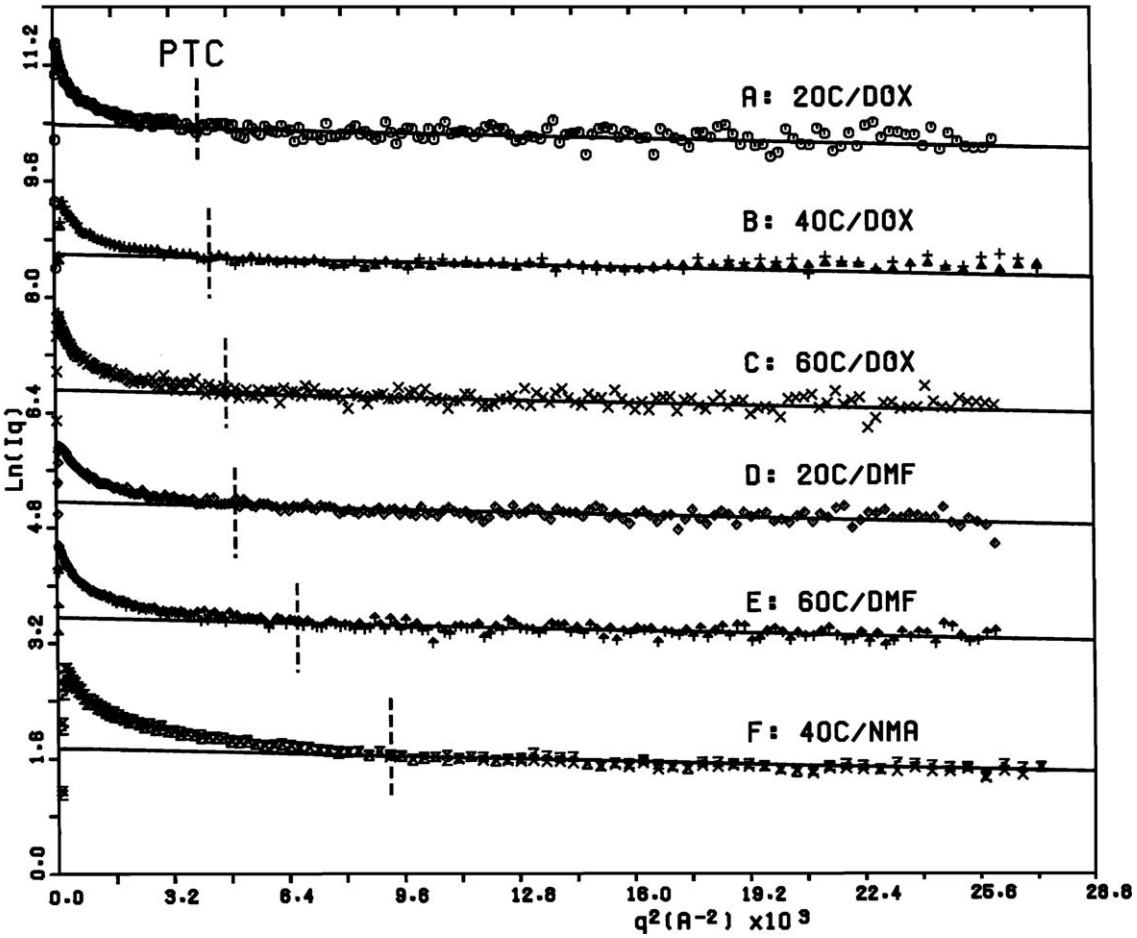

Fig. 2. The plot of $\ln(I(q)q)$ vs. q^2 for PTC: (A) 20 °C in DOX, C_p=0.69 g/dl (○); (B) 40 °C in DOX, C_p=1.00 g/dl (△), C_p=0.50 g/dl (+); (C) 60 °C in DOX, C_p=0.69 g/dl (×); (D) 20 °C in DMF, C_p=0.71 g/dl (◊); (E) 60 °C in DMF, C_p=0.71 g/dl (▲); (F) 40 °C in NMA, C_p=1.00 g/dl (⊠), C_p=0.50 g/dl (Z). A vertical dotted line designates the transition point q^{*2} between Debye-region and Porod-region, which was decided in Fig. 3-(2).

transition point q^* between Debye-region and Porod region is related to P_l:

$$P_l = \frac{A}{q^*}, \tag{15}$$

where A is a constant. Method-II was applied to evaluate P_l for CTC in DOX [8] and for PL in water [20].

When the conditions Eqs. (13) and (14) are satisfied and value A in Eq. (15) is properly assigned, two values of P_l evaluated by Methods-I and -II should coincide with each other. As is shown below, two values of P_l for PTC as well as for PL were found to be almost equal when A is assigned to be 2.87, which was theoretically derived for a semiflexible chain by Burchard and Kajiwara [21].

4. Results and discussion

In Fig. 1, temperature T(°C) dependence of $[\eta]$ (dl/g) is shown in the form of $(2/3)\ln[\eta]$ vs. T for PTC, ATC and CTC in DOX solution (○) and DMF solution (△). It is clear that $[\eta]$ for all samples significantly decreases with raising the temperature, indicating that not only ATC and CTC but also PTC exhibits the thermal-induced conformational transition.

As is well established, $[\eta]$ is related to $\langle R_g^2\rangle$ as follows:

$$[\eta] \propto \frac{\langle R_g^2\rangle^{\frac{3}{2}}}{M} \propto \frac{\alpha^3 \langle R_g^2\rangle_0^{\frac{3}{2}}}{M}, \tag{16}$$

where $\langle R_g^2\rangle_0$ is $\langle R_g^2\rangle$ at an unperturbed state and α expansion factor. From Eq. (16), the temperature dependence of $[\eta]$ is expressed by:

$$\frac{2}{3}\frac{\partial \ln[\eta]}{\partial T} = \frac{\partial \ln\langle R_g^2\rangle}{\partial T} = \frac{\partial \ln\alpha^2}{\partial T} + \frac{\partial \ln\langle R_g^2\rangle_0}{\partial T} \tag{17}$$

For a wormlike chain, $\langle R_g^2\rangle_0$ is given in terms of P_l and contour length of a chain L [22]:

$$\langle R_g^2\rangle_0 = \frac{1}{3}P_l L - P_l^2 + \left(\frac{2P_l^3}{L}\right)\left\{1 - \frac{P_l}{L}\left(1 - \exp\left(-\frac{L}{P_l}\right)\right)\right\} \tag{18}$$

From Eqs. (17) and (18), the temperature dependence of $[\eta]$ would indicate that P_l or α^2 or both should depend on the temperature. The temperature dependence of P_l for PTC and ATC was studied below by analyzing the SAXS data.

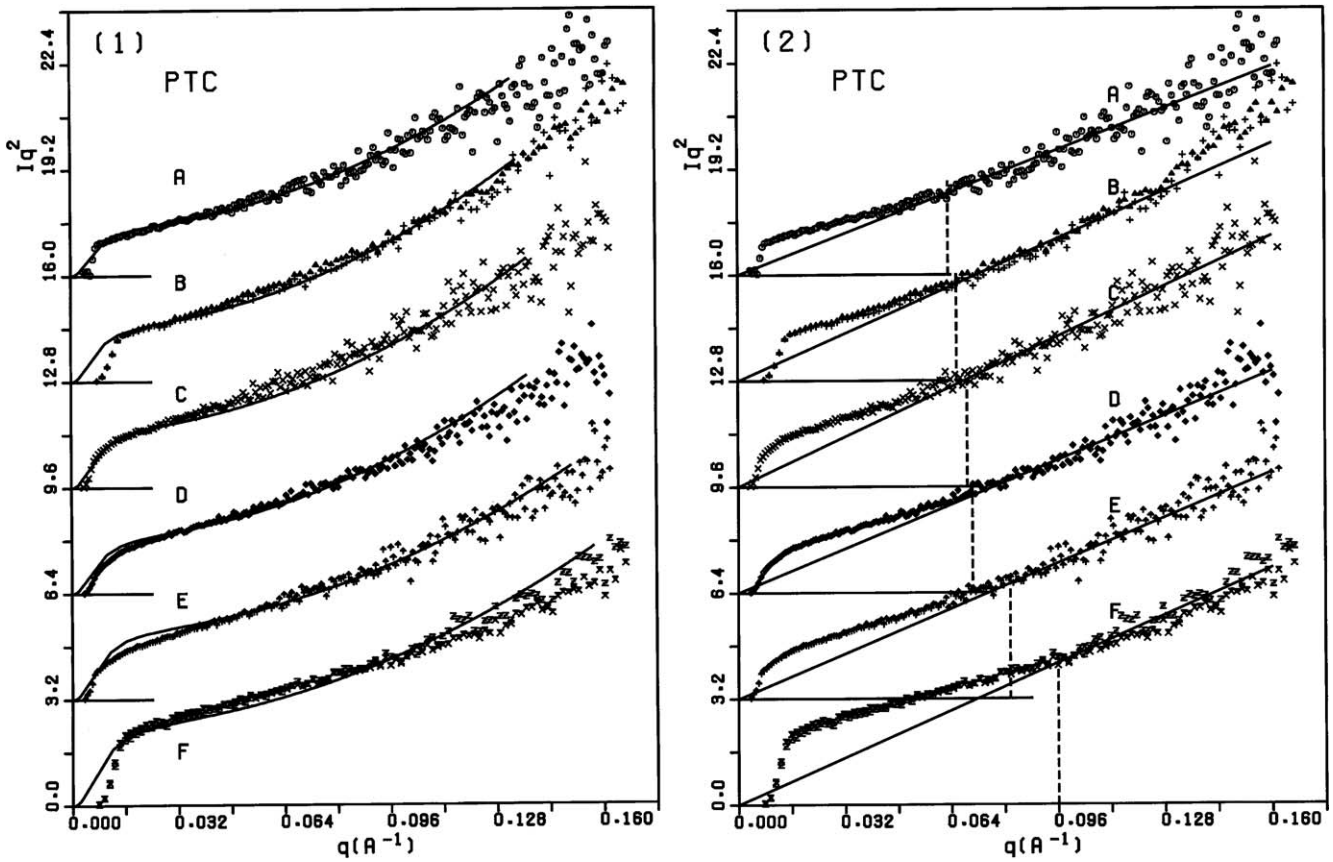

Fig. 3. -(1) The Kratky plot $I_{thin}(q)q^2$ vs. q for PTC, where symbols in the figure have the same meanings as those in Fig. 2. Solid curve is a scattering function $P(\theta)$ for a wormlike chain, which was computed by Eq. (10) with P_l: (A) 45, (B) 44, (C) 42, (D) 42, (E) 35 and (F) 32 Å and the contour length L ~2040 Å. -(2) The Kratky plot $I_{thin}(q)q^2$ vs. q for PTC, where symbols in the figures have the same meanings as those in Fig. 2. A vertical dotted line shows the transition point q^* between the Debye-region and Porod-region. When evaluated with q^*, P_l is (A) 45, (B) 44, (C) 42, (D) 41, (E) 35 and (F) 30 Å.

Fig. 2 shows the plots of $\ln(I(q)\,q)$ vs. q^2 for PTC: (A) 20 °C in DOX; (B) 40 °C in DOX; (C) 60 °C in DOX; (D) 20 °C in DMF; (E) 60 °C in DMF; (F) 40 °C in NMA. The meaning of the symbols in the figure is given in the figure caption. The data points for different samples begin to show linearity at different q, depending on the temperatures or solvents, indicating that the chain flexibility of PTC depends on these factors. In performing the linear fit, we have taken into account necessary conditions that the linear region should begin to appear around q^* in Eq. (15), which is more easily determined from the corresponding Kratky plot and, moreover, Eq. (9) should be satisfied in that linear q^2 range.

$\langle R_{cs}^2\rangle^{1/2}$ for PTC is listed in Table 1. With $\langle R_{cs}^2\rangle$and P_l, which is obtained later, it was confirmed that Eq. (9) is well satisfied in the linear q^2 range in Fig. 2. In the figure, two data in (B) at $C_p=1.00$ (△) and 0.50 g/dl (+), and two data in (F) at $C_p=1.00$ (⧖) and 0.50g/dl (Z) could be overlapped to form a single scattering curve by shifting one of the two data along the ordinate. From this observation and since C_p is sufficiently lower than the corresponding C_p^* (Table 1), it is safely assumed that $I(q)$ for all samples would reflect intramolecular-interferences within an isolated chain, except in the extremely small q range.

Fig. 3-(1) and -(2) shows the Kratky plots $I_{thin}(q)q^2$ vs. q for PTC, where symbols in the figures have the same meanings as those in Fig. 2. In Fig. 3-(1), the data was analyzed with Method-I, i.e. by comparing the observed data with $P(\theta)$ for the wormlike chain model, Eq. (10). The best P_l was assigned by trial-and-error under the conditions Eqs. (13) and (14), where L was evaluated to be 2040 Å from $M_v=2.12\times10^5$ and the projection of a virtual bond length l onto the persistence length direction, 5.0 Å [9]. Solid curves in the figure are the theoretical curves thus obtained, where P_l is : (A) 45±3, (B) 44±3, (C) 42±3, (D) 42±3, (E) 35±3 and (F) 32±3 Å (Table 1). Downward deviation of the data from the theoretical curve in a low q range$<\sim0.016$ Å^{-1} would be due to a limited small-angle resolution and effect of polydispersity of the sample (M_w/M_n ~1.2), whereas downward deviation in a high q range$>\sim0.12$ Å^{-1} would reflect that the condition Eq. (14) is no longer satisfied in the q range. In all samples, P_l thus obtained has satisfied Eq. (13).

In Fig. 3-(2), the data for PTC is analyzed with Method-II. It is seen that the data in a high q range is well on a straight-line (solid line) passing through an origin, showing the q range is the Porod-region, but the data begins to deviate upward from the

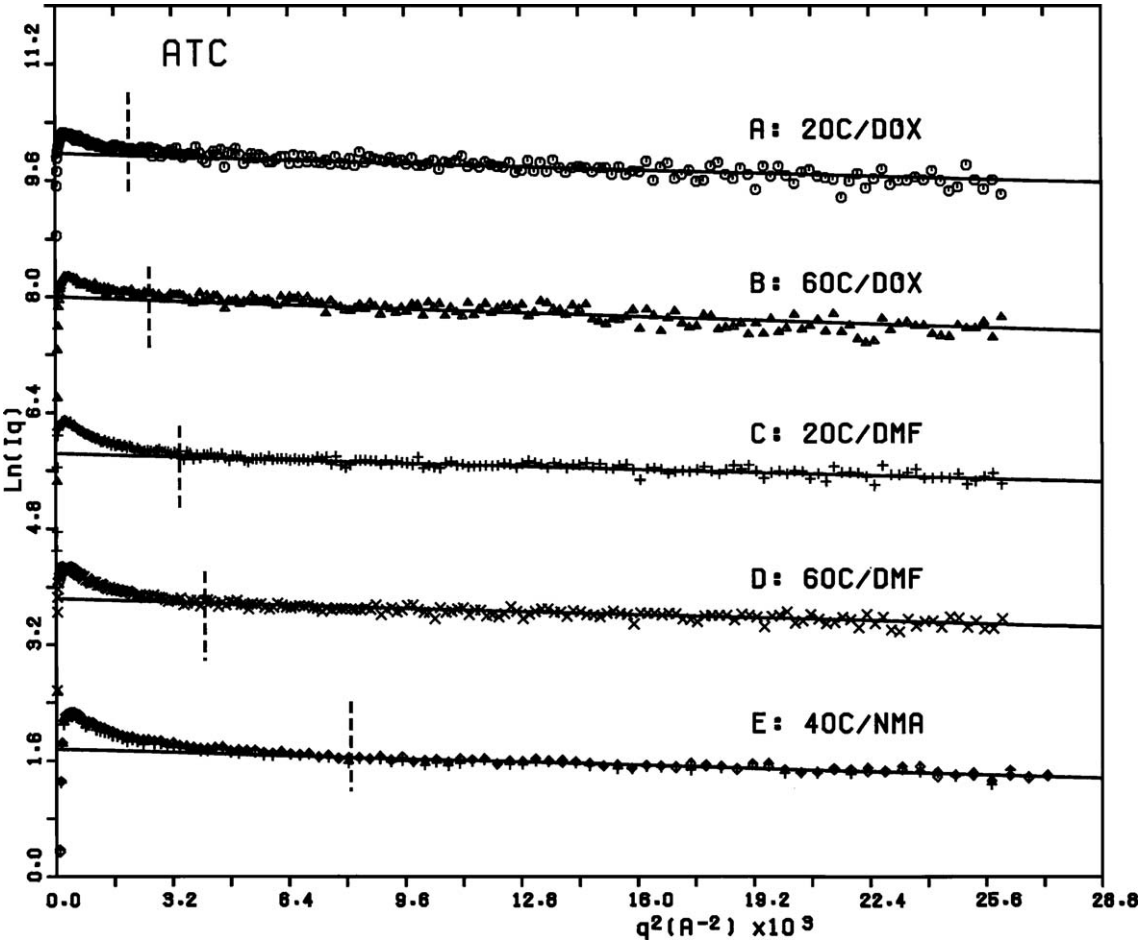

Fig. 4. The plot of $\ln(I(q)q)$ vs. q^2 for ATC: (A) 20 °C in DOX, $C_p=1.10$ g/dl (○); (B) 60 °C in DOX, $C_p=1.10$ g/dl (△); (C) 20 °C in DMF, $C_p=1.00$ g/dl (+); (D) 60 °C in DMF, $C_p=1.00$ g/dl (×); (E) 40 °C in NMA, $C_p=1.00$ g/dl (◊), $C_p=0.50$ g/dl (▲). A vertical dotted line designates the transition point q^{*2} between Debye-region and Porod-region, which was decided in Fig. 5.

line as q is decreased. Transition point q^* (dotted line) between Debye-region and Porod region was assumed to be equal to q where the deviation appears. Substituting q^* and $A=2.87$ into Eq. (15), P_l is evaluated to be (A) 45±3, (B) 44±3, (C) 42±3, (D) 41±3, (E) 35±3 and (F) 30±3 Å (Table 1), which well agrees with those evaluated by Method-I. q^{*2} thus obtained is also marked by a dotted line in Fig. 2, where it is seen that the data points show a good linearity in a range of q^2 higher than q^{*2}.

Fig. 4 shows the plot of $\ln(I(q)q)$ vs. q^2 for ATC: (A) 20 °C in DOX; (B) 60 °C in DOX; (C) 20 °C in DMF; (D) 60 °C in DMF; (E) 40 °C in NMA, where two data in (E) at $C_p=1.00$ (◇) and 0.50g/dl (▲) were overlapped. The resultant $\langle R_{cs}^2\rangle^{1/2}$ is listed in Table 1 and the Kratky plot $I_{thin}(q)q^2$ vs. q is shown in Fig. 5. Here, the condition Eq. (13) was not satisfied for any samples and thus the SAXS data was analyzed with Method-II only. In Fig. 5, the transition point q^* between Porod-region and Debye-region is marked by a dotted line. With q^* and $A=2.87$, P_l is estimated to be (A) 64±3, (B) 56±3, (C) 49±3, (D) 45±3 and (E) 32±3 Å (Table 1). In Fig. 4, q^{*2} is marked by a dotted line.

The result in Table 1 clearly shows that P_l for both PTC and ATC decreases as the temperature is raised and P_l in DOX > P_l in DMF > P_l in NMA and P_l of ATC > P_l of PTC as far as they are compared at the same temperature and solvent. These results may suggest that intramolecular hydrogen bonds are formed between carbanilate groups neighboring along the backbone chain. In order to confirm the validity of the suggestion, therefore, our attention was directed to examining whether P_l for PL having no carbanilate groups is independent of the temperature and solvent.

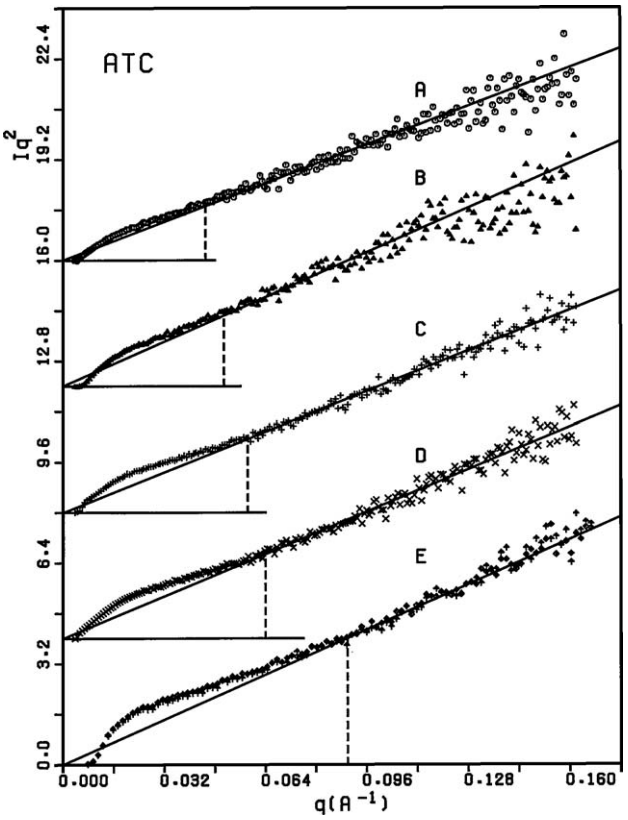

Fig. 5. The Kratky plots for ATC, where symbols in the figures have the same meanings as those in Fig. 4. A vertical dotted line shows the transition point q^* between the Debye-region and Porod-region. When evaluated with q^*, P_l is (A) 64, (B) 56, (C) 49, (D) 45 and (E) 32 Å.

Fig. 6 shows the plot of $\ln(I(q)q)$ vs. q^2 for PL: (A) 25 °C in WAT; (B) 25 °C in DMF; (C) 60 °C in DMF, where two data in (A) at $C_p=0.50$ (○) and 1.00 g/dl (△) were overlapped. The data points begin to show a linearity at a higher q^2 compared with PTC (Fig. 2) or ATC (Fig. 4), indicating that PL is a more flexible chain than PTC or ATC. The resultant $\langle R_{cs}^2\rangle^{1/2}$ was roughly estimated to be 5.1±1.0 Å (Table 1) under all conditions, which was larger than that for unsolvating molecule, 2.3 Å [23]. In Fig. 7-(1), the Kratky plot $I_{thin}(q)q^2$ vs. q for PL is compared with $P(\theta)$ (solid curve)of a wormlike chain with P_l of 23±3 Å for all samples (Table 1), where the contour length L ~3086 Å was evaluated from $M_v=1.0\times10^5$ and $l=5.0$ Å [9]. In Fig. 7-(2), it is shown that the transition point q^* is decided as is marked by a dotted line, and from q^* ~0.13 Å^{-1} and $A=2.87$, P_l was roughly evaluated as 22±4 Å for all samples (Table 1), which is in agreement with P_l evaluated with Method-I.

To be noted here, PL is so flexible and the linear regions for PL in Figs. 6 and 7-(2) are so limited that $\langle R_{cs}^2\rangle^{1/2}$ and P_l for PL, especially for data (C), in Table 1 would include comparatively larger error. As is shown in (D) in Figs. 6 and 7-(2), however, the plots for all data (A), (B) and (C) could be satisfactorily overlapped to form a single curve, at least, except in extremely small q region, by shifting them along the ordinate and by multiplying them by a factor, respectively. This result would show that the local conformation of PL, characterized by $\langle R_{cs}^2\rangle^{1/2}$ and P_l, is substantially independent of temperature and solvent and thus the temperature and solvent dependence of P_l for PTC and ATC would be due to the intramolecular hydrogen-bonds formed between the carbanilate groups.

With P_l given in Table 1, $\langle R_g^2\rangle_0$ for PTC and ATC was computed by Eq. (18), assuming that the sample has monodispersed molecular-weight of M_v and L can be estimated from M_v, together with $l=5.0$ [9] and 4.4 Å [24], respectively. Dayan et al. [25] have indicated that, for CTC with molecular-weight distribution of Schulz type, calculations assuming a monodispersed sample of M_v and $[\eta]$ give a good approximation for P_l. The computational results, after shifting along the ordinate, are shown in Fig. 1 by symbol square (□) in DOX solution and crosses (×) in DMF solution, where solid a line is drawn as a guide to see the tendency shown by each data set. It is clearly shown that the temperature-dependence of $\langle R_g^2\rangle_0$ well agrees with that of $[\eta]$. As a consequence, it is concluded that the conformational transition of PTC and ATC is ascribed to a change of P_l and the excluded-volume effect would be negligible or invariable, at least, in the molecular-weight range of the samples employed.

Such a change of P_l with temperature is consistently understood if there exists a scheme that intramolecular hydrogen bonds are formed between carbanilate groups neighboring along the backbone chains, but they are gradually and cooperatively collapsed as the temperature is raised. This

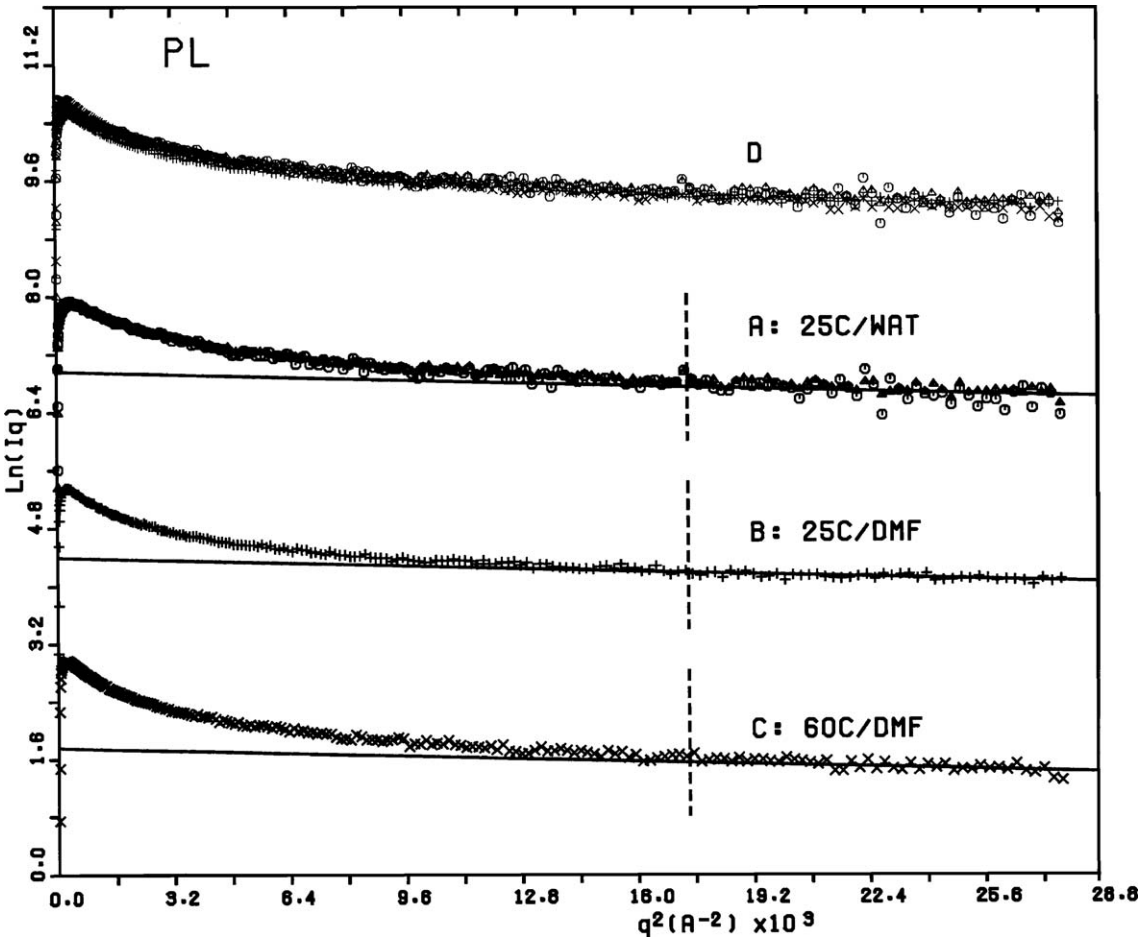

Fig. 6. The plot of $\ln(I(q)\,q)$ vs. q^2 for PL: (A) 25 °C in WAT, C_p=0.50 g/dl (○), C_p=1.00 g/dl (△); (B) 25 °C in DMF, C_p=1.00 g/dl (+); (C) 60 °C in DMF, C_p=1.00 g/dl (×). A vertical dotted line designates the transition point q^{*2} between Debye-region and Porod-region, which was decided in Fig. 7-(2). In D, all data (A)~(C) are overlapped to form a single curve by shifting them along the ordinate.

scheme is supported by the studies [4] on the physical properties relating to the overall chain-dimension of ATC and CTC.

5. Concluding remarks

The thermal-induced conformational transition for PTC and ATC from an expanded form to a compact form was clarified from the temperature dependence of $[\eta]$ in the temperature domain of 20 to 60 °C. It was shown that P_l decreases as the conformational transition proceeds and the temperature dependence of $[\eta]$ is well elucidated in terms of temperature-dependent P_l with the wormlike chain model. From the results, it is suggested that intramolecular hydrogen bonds would be formed between carbanilate groups neighboring along the backbone chain, but they are gradually and cooperatively collapsed as the temperature is raised, inducing the conformational transition.

References

[1] A.K. Gupta, E. Marchal, W. Burchard, Effect of temperature on the flexibility of cellulose tricarbanilate in dioxane and ethyl acetate by dielectric measurements, Macromolecules 8 (1975) 843–849.

[2] A.K. Gupta, E. Marchal, W. Burchard, B. Pfannemuller, Dielectric study of amylose tricarbanilate in dioxane and ethyl acetate, Macromolecules 12 (1979) 281–284.

[3] J.M.W. Noordermeer, R. Daryanani, H. Janeschitz-Kriegl, Flow birefringence studies of polymer conformation: cellulose tricarbanilate in two characteristic solvents, Polymer 16 (1975) 359–369.

[4] W. Sutter, W. Burchard, Comparative study of the hydrodynamic properties of cellulose and amylose tricarbanilates in dilute solutions Viscosity, sedimentation and diffusion measurements in 1,4-dioxane in the molecular weight range of $500 \leqq M \leqq 5 \cdot 10^6$, Makromol. Chem. 179 (1978) 1961–1980.

[5] J. Danhelka, M. Netopilik, M. Bohdanecky, Solution properties and chain conformation characteristics of cellulose tricarbanilate, J. Polym. Sci., Polym. Phys. Ed. 25 (1987) 1801–1815.

[6] B. Hsu, C.A. McWherter, D.A. Brant, W. Burchard, Analysis of cooperative conformational transitions in cellulose and amylose tricarbanilates, Macromolecules 15 (1982) 1350–1357.

[7] W.G. Miller, P.J. Flory, Dimensions of polypeptide chains in helicogenic solvents, J. Mol. Biol. 15 (1966) 298–314.

[8] A.K. Gupta, J.P. Cotton, E. Marchal, W. Burchard, H. Benoit, Persistence length of cellulose tricarbanilate by small-angle neutron scattering, Polymer 17 (1976) 363–366.

[9] T. Kato, T. Okamoto, T. Tokuya, A. Takahashi, Solution properties and chain flexibility of pullulan in aqueous solution, Biopolymers 21 (1982) 1623–1633.

[10] W. Burchard, E. Husemann, Eine vergleichende Strukturanalyse von cellulose- und amylose-tricarbanilaten in Losung, Makromol. Chem. 44–46 (1961) 358–387.

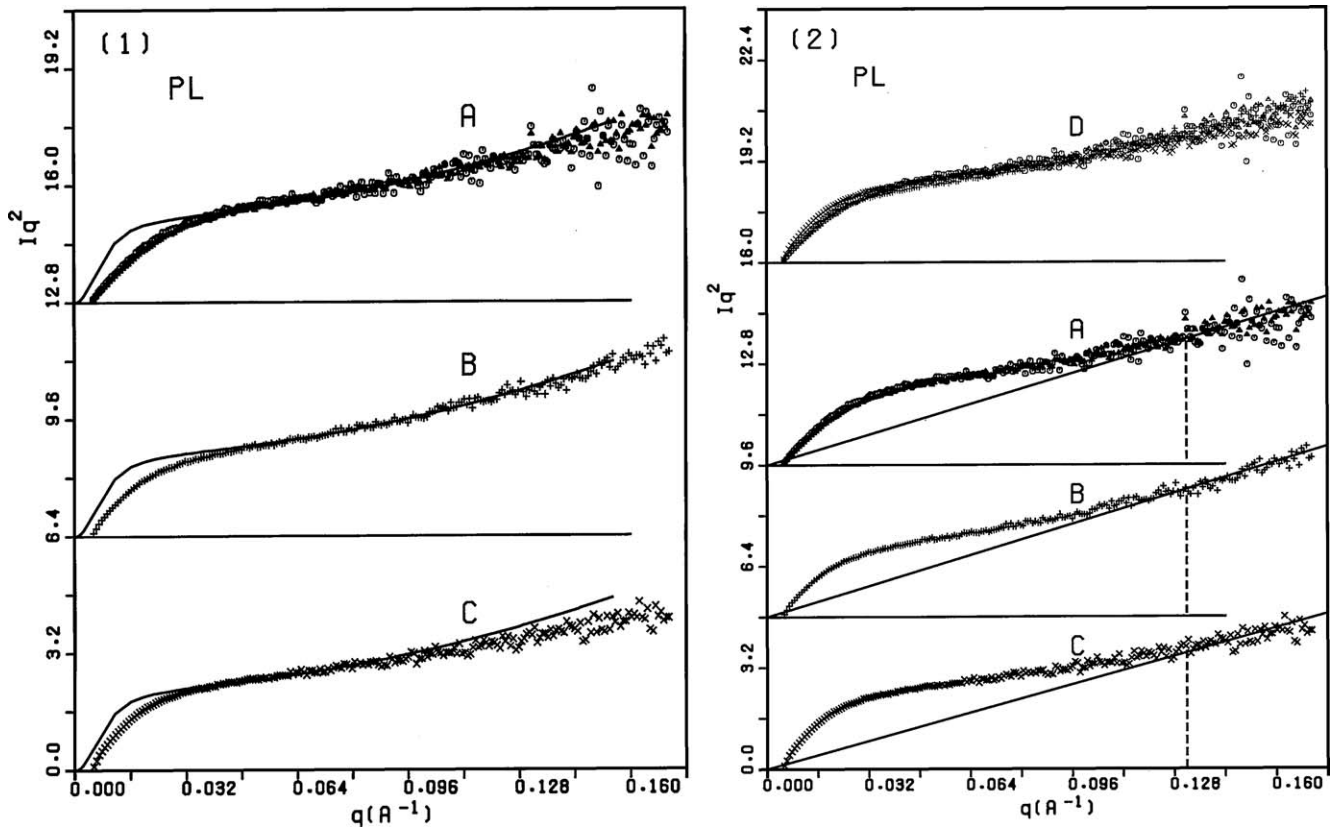

Fig. 7. (1) The Kratky plot $I_{thin}(q)q^2$ vs. q for PL, where symbols in the figures have the same meanings as those in Fig. 6. Solid curve is a scattering function $P(\theta)$ for a wormlike chain, which was computed by Eq. (10) with P_l: (A) 23, (B) 23 and (C) 23 Å, where the contour length L ~3086 Å. (2) The Kratky plot $I_{thin}(q)q^2$ vs. q for PL, where symbols in the figures have the same meanings as those in Fig. 6. A vertical dotted line shows the transition point q^* between the Debye-region and Porod-region. When evaluated with q^*, P_l is (A) 22, (B) 22 and (C) 22 Å. In D, all data (A)~(C) are overlapped to form a single curve by multiplying them by a factor.

[11] A. Sugano, Graduation thesis, Mie University, 1983.
[12] T. Ueki, Y. Hiragi, Y. Izumi, H. Tagawa, M. Kataoka, Y. Muroga, T. Matsushita, Y. Amemiya, Photon Factory Activity Report (1982/1983). VI70–VI71
[13] P.G. de Gennes, Scaling Concept in Polymer Physics, Cornell University Press, Ithaca, New York, 1979, pp. 76–77.
[14] Y. Muroga, I. Noda, M. Nagasawa, Investigation of local conformations of polyelectrolytes in aqueous solution by small-angle X-ray scattering: 1. Local conformations of poly(sodium acrylates), Macromolecules 18 (1985) 1576–1579.
[15] G. Porod, in: O. Glatter, O. Kratky (Eds.), Small Angle X-ray Scattering, Academic Press, New York, 1982, pp. 32–35.
[16] P. Sharp, V.A. Bloomfield, Light scattering from wormlike chains with excluded volume effects, Biopolymers 6 (1968) 1201–1211 (with a correction in C. W. Schmid, F. P. Rinehart, J. E. Hearst, Biopolymers 10 (1971) 883–893).
[17] Y. Muroga, T. Yoshida, S. Kawaguchi, Conformation of poly(methacrylic acid) in acidic aqueous solution studied by small angle X-ray scattering, Biophys. Chem. 81 (1999) 45–57.
[18] Y. Muroga, S. Iida, S. Shimizu, H. Ikake, K. Kurita, Conformation of poly (sodium ethacrylate) in solution studied by small-angle X-ray scattering, Biophys. Chem. 110 (2004) 49–58.
[19] O. Kratky, Possibilities of X-ray small-angle analysis in the investigation of dissolved and solid high-polymer substances, Pure Appl. Chem. 12 (1966) 483–523.
[20] Y. Muroga, Y. Yamada, I. Noda, M. Nagasawa, Local conformation of polysaccharides in solution investigated by small-angle X-ray scattering, Macromolecules 20 (1987) 3003–3006.
[21] W. Burchard, K. Kajiwara, The statistics of stiff chain molecules I. The particle scattering factor, Proc. R. Soc. Lond., A 316 (1970) 185–199.
[22] H. Benoit, P. Doty, Light scattering from non-gaussian chains, J. Phys. Chem. 57 (1953) 958–963.
[23] G.M. Pavlov, E.V. Korneeva, N.P. Yevlampieva, Hydrodynamic characteristics and equilibrium rigidity of pullulan molecules, Int. J. Biol. Macromol. 16 (1994) 318–323.
[24] S. Arnott, W.E. Scott, Accurate X-ray diffraction analysis of fibrous polysaccharides containing pyranose rings: Part 1. The linked-atom approach, J. Chem. Soc., Perkin Trans. 2 (1972) 324–335.
[25] S. Dayan, P. Maissa, M.J. Vellutini, P. Sixou, Intrinsic viscosity of cellulose derivatives and the persistent cylinder model of Yamakawa, Polymer 23 (1982) 800–804.